A&A 458, 1007–1011 (2006)
DOI: 10.1051/0004-6361:20064971

Astronomy & Astrophysics

The size distribution of asteroids in cometary orbits and related populations

A. Alvarez-Candal[1] and J. Licandro[2,3]

[1] Observatório Nacional/MCT. Rua Gal. José Cristino 77, Rio de Janeiro, 20921-400, RJ, Brazil
e-mail: alvarez@on.br
[2] Isaac Newton Group, PO Box 321, 38700, Santa Cruz de la Palma, Tenerife, Spain
e-mail: licandro@ing.iac.es
[3] Instituto de Astrofísica de Canarias, c/vía Láctea s/a, 38205, La Laguna, Tenerife, Spain

Received 6 February 2006 / Accepted 4 August 2006

ABSTRACT

Aims. In this work we study the cumulative size distribution of the population of asteroids in cometary orbits (ACOs), aiming to discriminate its cometary or asteroidal origin.
Methods. The cumulative luminosity function was determined based on the absolute magnitudes of the ACOs. The cumulative size distribution was then derived and compared to that of possible sources of ACOs, such as the Trojans and Hilda asteroids and Jupiter family comets. The size distribution of the two sub-populations, NEOs and non-NEOs, identified by Licandro et al. (2005) were also analyzed.
Results. The derived cumulative size distribution index of the ACO population is 2.55 ± 0.04. The two subpopulations have distinct indexes: -2.20 ± 0.04 and -2.45 ± 0.04 for the NEOs and non-NEOs, respectively. The first value is similar to that of the Trojans and Hilda asteroids and the second to the Jupiter family comets.
The obtained values suggest that the non-NEO sub-population of ACOs can be composed of a significant fraction of dormant Jupiter family comets. On the other hand, the NEO sub-population is mostly formed by scattered objects from diverse sources, including main belt asteroids.

Key words. minor planets, asteroids – comets: general

1. Introduction

It has been assumed that comets and asteroids form two distinct classes of small objects of the Solar System. Comets are planetesimals formed during the early ages of the Solar System in a region that extends from the giant planets to slightly beyond the limits of the pre-solar nebula. Even if they have been processed in some ways, comets and other related icy minor planets like trans-neptunian objects (TNOs) and Centaurs are the most pristine observable objects from that period. On the other hand, asteroids were formed in the region between Mars and Jupiter.

As a consequence of the different formation regions, the volatile content of the two populations is different. This fact has provided the most apparent distinction between members of the two populations: comet nuclei, when close to the Sun, are usually surrounded by a coma produced by the out-gassing of volatiles, caused by solar heating, while asteroids are not. This simple distinction is questioned by the following arguments: *(i)* the discovery of icy objects (TNOs and Centaurs) that rarely develop a coma due to their distance from the Sun; *(ii)* the discovery of asteroids with dynamical properties similar to those of comets; *(iii)* the realization that comets might develop an asteroidal appearance when sublimation stops, either due to the depletion of volatile materials or by the growth of a surface crust of refractory material up to a thickness that prevents subsurface volatiles from warming up to sublimation temperature (Rickman et al. 1990); *(iv)* the discovery of objects in typical asteroidal orbits that present temporary comet-like activity, e.g., (4015) Wilson-Harrington and (7968) Elst-Pizarro, or that have associated meteor showers that suggest some past cometary activity such as (3200) Phaeton.

The criterion used to define the sample of asteroids in cometary orbits is related to the Tisserand parameter (Kresák 1979), which is defined by the relation, $T = a_J/a + 2\cos I\sqrt{(a/a_J)(1-e^2)}$, where a and a_J are the semi-major axes of the orbits of the asteroid and Jupiter, respectively, while e and I are the eccentricity and the inclination of the asteroid's orbit. Note that I is measured relative to the orbital plane of Jupiter. By this criterion, cometary orbits are defined as those having $T < 3$, while asteroidal orbits are those with $T > 3$. Therefore, all the objects with $T < 3$ that do not present any signature of cometary activity are defined as asteroids in cometary orbits (ACOs). The orbits of those objects are dynamically unstable, implying that the population needs to be continually replenished. This in turn implies that there should be some dynamical mechanism that perturbs the orbit of typical asteroids changing their Tisserand invariant and/or some physical mechanism that deactivates comet nuclei, transforming a typical active comet into an object with a typical asteroidal appearance. Therefore, ACOs are good candidates to be extinct or dormant comets. Determining the fraction of dormant comets in the ACO population will thus provide important information for understanding the dynamics of the main belt and the end states of comet nuclei. In particular, the contribution of dormant comets to the population of near Earth objects (NEOs) has been studied by different authors using dynamical considerations and with very different results (e.g. Bottke et al. 2002; Fernández et al. 2002).

We restrict the following analysis to objects with $2 \leq T \leq 3$, which is the common range of Tisserand parameter of Jupiter family comets (JFCs). Dormant comets in this population should proceed from the JFC, whose physical properties are better known than for other comets. Objects with $T < 2$ are usually called *Damocloids* (Jewitt 2005) and are asteroids in Halley-type cometary orbits. The properties of Damocloids will not be discussed here due to the small number of known objects. It is also worth noting that objects such as Trojans, Hildas, or Cybeles are excluded from our ACO population definition, even though some of them have $T < 3$.

In past years, diverse studies have searched for physical correlations among the population of comets and ACOs, but they lack in detailed information about the comet nuclei. Until recently the only certain information was that comets present slightly red, featureless spectra, similar to D-type asteroids (e.g., Jewitt 2002; Licandro et al. 2002). Nevertheless, recent results for albedos and spectra indicate that they have some intrinsic properties that are not shared by other asteroid populations. Analyzing a sample of ACOs, Fernández et al. (2005) found that objects with $T < 2.6$ tend to have small albedo, much like comet nuclei, while the transition regions ($T \sim 3$) have a wider spread in albedo values. Licandro et al. (2005) found differences in the spectroscopic properties of two sub-samples of ACOs, the NEOs with $q \leq 1.3$ AU and the non-NEOs. In this paper we study the cumulative luminosity function (CLF) and cumulative size distribution (CSD) of those sub-populations trying to explore their possible origin.

In the next section we describe the relationship between both distributions, and in Sect. 3 we discuss the NEO and non-NEO sub-populations and the criteria used to define the analyzed sample. A brief discussion and a comparison with related populations are presented in Sect. 4. Finally in Sect. 5 the main results of the work are discussed.

2. Cumulative luminosity function and size distribution

A very important physical property of a population of minor planets is its CSD, which is related to its composition, as well as its collisional and dynamical evolution. The comparison of the CSD of asteroids in cometary orbits with that of possible sources can give important clues to the origin of the population or help to put some constraints on the possible contributions. It is particularly interesting to compare our results to the distribution of Jupiter family comets (Fernández et al. 1999; Tancredi et al. 2006), along with small and/or unstable Trojan asteroids (Jewitt et al. 2000; Yoshida & Nakamura 2005; Melita et al. 2006), and small Hilda asteroids.

The CSD can be derived from the CLF defined as

$$\log\left[N_H(< H)\right] = \mathbb{C} + \gamma H, \tag{1}$$

where $N_H(<H)$ is the number of objects with an absolute visual magnitude lower than H, while $\mathbb{C}$ and γ are constants to be determined. Note that H is related to the radius R of the object by

$$\log\left[p_V \pi R^2\right] = 16.85 + 0.4(m_\odot - H) \tag{2}$$

where R is given in km and $m_\odot = -26.77$ is the apparent V-magnitude of the Sun.

Equation (1) can be written as

$$H \propto \log\left[N_H(<H)^{1/\gamma}\right].$$

From Eq. (2), and assuming a constant albedo p_V, we then have

$$H \propto \log\left[R^{-5}\right].$$

Equating the above relations and taking into account that $N_H(<H) \Rightarrow N_R(>R)$, we obtain

$$N_R(>R) \propto R^{-5\gamma}. \tag{3}$$

Note that in the above equation the value -5γ is usually known as the CSD index, s.

3. Results

In what follows the term featureless refers to objects with a linear visible spectra, representative of C-, B-, F-, D-, and X-type taxonomic classifications. Objects with a strong 1 μm band, i.e., of the S-, A-, V-, and Q-types, are denominated as featured.

3.1. The near-Earth objects sample

Licandro et al. (2005) noticed that most of the featured ACOs belong to the NEO population, while the non-NEO are mostly featureless. As the ACOs are dynamically unstable and the population needs to be continually replenished by main belt asteroids and/or dormant comets, the mineralogical difference observed between the NEO and non-NEO sub-populations should be indicative of differences in their refilling mechanism. The abundance of featured objects in the NEO population seems to indicate that it is composed of a significant fraction of asteroids dynamically scattered from the inner main belt. On the other hand, the non-NEO population should be mostly replenished by dynamically scattered asteroids from the outer main belt and/or dead comet nuclei. Below we, therefore, consider the NEO and the non-NEO, sub-populations separately.

3.2. Interlopers

Licandro et al. (2005) noticed that in a sample of ACO spectra, all the featured spectra have $T \geq 2.9$. This suggests that ACOs scattered from the inner main belt are not very abundant for $T < 2.9$, while those with $2.9 \leq T \leq 3$ are contaminated by a large fraction of "interlopers" from the inner main belt.

It was also pointed out by Fernández et al. (2005) that ACOs with $T < 2.6$ tend to have lower albedo and less dispersion than objects with $2.6 \leq T < 3$. This also supports the idea that interlopers are abundant in the group of ACOs with $2.9 \leq T \leq 3.0$. To investigate this point we compared the distribution of the Tisserand parameter in the ACO and JFC populations (Fig. 1). The former presents a much larger fraction of objects with $T > 2.9$ than do comets, confirming the previous conclusion. Therefore, we use only ACOs with $T < 2.9$ to construct the distribution. In this way the fraction of featured objects is minimized, and only those with cometary-like spectrum are considered.

3.3. Bias analysis

The CLF was derived using the absolute magnitude, H, of ACOs from the data available at Lowell Observatory[1]. In view of the

[1] ftp://ftp.lowell.edu/pub/elgb/astorb.dat

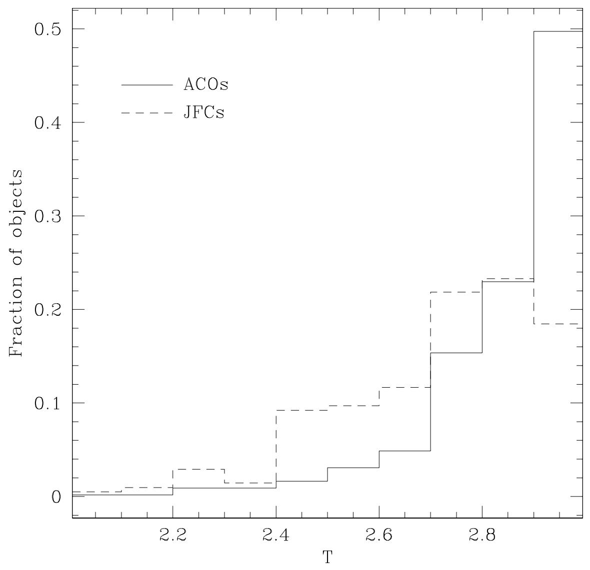

Fig. 1. Normalized distributions of the Tisserand parameter, T of ACOs (continuous line, 624 objects), and JFCs (dashed line, 261 objects). The bin has a length 0.1 in T. It is clear the overabundance of ACOs with respect to JFCs in the last bin, that is a transition zone.

above considerations, we only consider those ACOs with $2 < T \leq 2.9$.

Another problem, discussed in Fernández et al. (1999) and Tancredi et al. (2006), arises from the observational biases. It is easier to discover the larger ACOs and those that come closer to Earth. The first effect is visible in the distribution as a departure from the linear trend at a certain $H_{\rm limit}$ value.

As we are dealing with objects that move in JFC-like orbits, an easy way to deal with the second bias is to consider a sub-sample of objects with small perihelion distances as in Fernández et al. (1999) and Tancredi et al. (2006). We presume a higher degree of completeness for this sub-sample. Using the above criteria, 262 objects comprise the complete sample of ACOs up to $q \leq 2$ AU. The number of NEO objects are 151, while the non-NEOs are 111.

A third possible bias effect is the phase darkening, mostly due to the roughness of the objects' surface, and that accounts for a decrease of the magnitude while observing at large phase angles (see Kaasalainen et al. 2001). This mostly affects NEOs. In order to check whether this bias is affecting our sample, we used the discovering data from SPACEWATCH[2]. Figure 2 shows the absolute magnitude vs. the phase angle at the moment of the discovery of 521 NEOs (not necessarily in cometary orbits). There, H is computed following the $H-G$ system (Bowell et al. 1989). It is not clear from the figure how the phase darkening should be affecting our data since in the region of interest up to $H \sim 16.5$, the data seems fairly uniformly distributed.

3.4. Computing the cumulative distribution

The slope of the CLF depends critically on the range of magnitudes considered, since going too far into the faint tail will result in a shallow index, due to the incompleteness of the data. Therefore, it is important to determine a limit in magnitude ($H_{\rm limit}$) so as to fit Eq. (1). After many attempts, we defined $H_{\rm limit} \sim 15$ for both the complete sample of ACOs and the non-NEO sup-population. The $H_{\rm limit} \sim 16.5$ was defined for the

[2] http://spacewatch.lpl.arizona.edu/

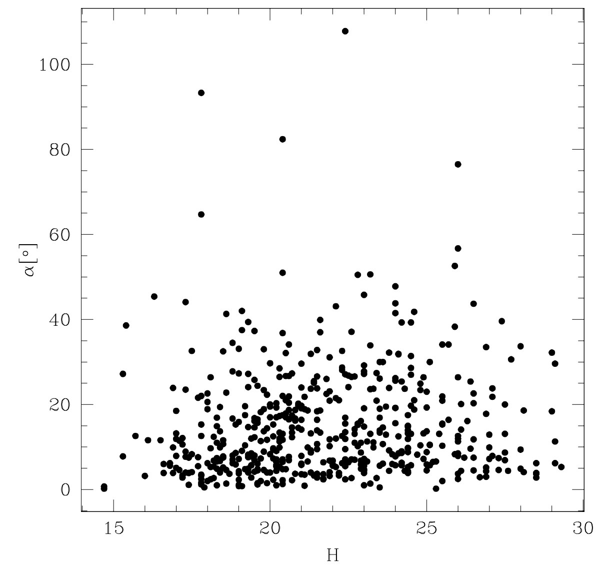

Fig. 2. Plot of H vs. α at the moment of discovery of 512 NEOs from SPACEWATCH.

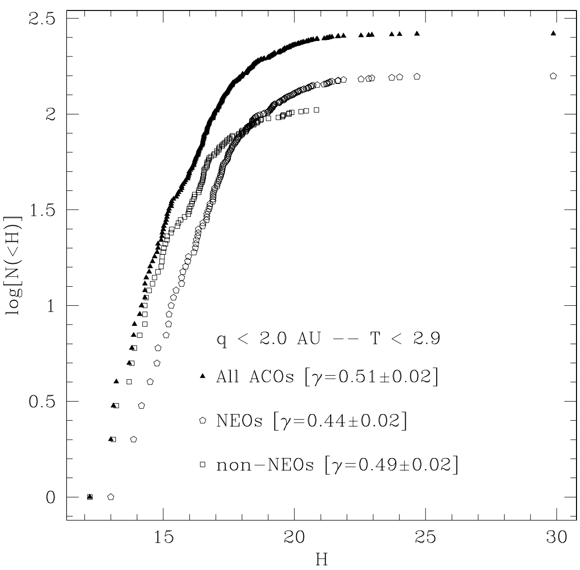

Fig. 3. Cumulative luminosity function of ACOs. The complete sample is shown with filled triangles, while the sub-populations are shown with open squares, non-NEOs, and open circles, NEOs.

NEOs. These are the values where the root mean square of the fit of Eq. (1) is minimized.

The distributions for the three samples considered here are shown in Fig. 3. Note that it includes only objects with $q \leq 2.0$ AU. To derive the slope γ of the distributions, we fitted Eq. (1) to the data as given in Tancredi et al. (2006). As the data points are unevenly distributed, with only a few points at both ends of the distribution, we fitted the CLF to a re-binned data set. This was computed as the mean over each 0.25 mag bin.

To estimate an error for the computed γ, we fitted Eq. (1) to a series of limit magnitudes about $H_{\rm limit}$. The distribution for the complete sample of ACOs was fitted to the values $H_{\rm limit}$ = 14.5, 15.0, and 15.5, obtaining $\gamma = 0.52$, 0.51, and 0.49, respectively. The adopted value is, therefore, $\gamma = 0.51 \pm 0.02$. The same procedure was used for the non-NEOs, obtaining $\gamma = 0.50$, 0.49, and 0.46, therefore adopting the value $\gamma = 0.49 \pm 0.02$.

For the sake of comparison, we followed the same procedure for a sample with limiting perihelion distance of 2.5 AU. Obtaining $\gamma = 0.46$, 042, 0.40 for the complete sample of ACOs and $\gamma = 0.44$, 0.40, and 0.37 for the non-NEO. This result is consistent with a lower level of completeness when considering larger perihelion distances.

In the case of the NEOs, $H_{\rm limit} \sim 16.5$, so the distribution was fitted using a linear relation up to a series of $H_{\rm limit} = 16.0$, 16.5, and 17.0, obtaining $\gamma = 0.46$, 0.44, and 0.42, respectively. Therefore, we adopt $\gamma = 0.44 \pm 0.02$. The indexes of the cumulative size distribution (Eq. (3)) are -2.45 ± 0.04 and -2.20 ± 0.04 for the NEO and non-NEO sub-populations, respectively. The diameter of the objects range from 3 meters to 10 kilometers, computed from Eq. (2), and assuming $p_V = 0.056$. This albedo is the weighted mean from Fernández et al. (2005) results.

4. Discussion

The ACO population seems to be separated into two different sub-populations, the NEOs that have a cumulative size index of −2.20, shallower than the canonical Dohnanyi index of −2.5. On the other hand, the non-NEOs that have $s = -2.45$, very similar to the Dohnanyi index. These diverse values of s for these sub-populations are probably indicative of a different composition and origins.

We compared the computed indexes to those from some populations commonly believed to be sources for the ACOs, such as the Hilda and Trojan asteroids, and the JFCs. We will restrict the discussion to results obtained within the most similar range of absolute magnitudes possible, since objects in a similar size range have, possibly, a comparable physical and/or collisional evolution.

Hildas: we computed the distributions for the Hilda asteroids following the same procedure as the ACOs. We considered as Hilda asteroids those objects with $3.7 < a < 4.2$ AU, $e < 0.4$, and $I < 20^{\rm o}$. For the magnitude range $12.5 \le H \le 14.5$ (Fig. 4), we obtained $s = -2.1 \pm 0.1$. Although the range of magnitudes is narrower, the index is very similar to that of ACOs in NEO orbits.
Since we could not apply any constraint to the perihelion distance, the computed s-index should be considered with caution since it can be affected by incompleteness. In this case the unbiased s-value could be higher. Di Sisto et al. (2005), analyzing the dynamical evolution of escapees from the 3:2 mean motion resonance, Hildas, found that most of those that are injected into a JFC-like orbit have $q > 2.5$ AU. They have not been taken into account in the estimated size distribution due to our criterion of minimizing the observational bias.

Trojans: recent works on the size distribution of small Trojans, using different samples, agree reasonably well about the s-index. Jewitt et al. (2000) obtained $s = -2.0$. Yoshida & Nakamura (2005), studying the faint distribution of the L4 Trojans, obtained $s = -1.9$ for the magnitude range $14 \le H \le 18$. Using dynamical considerations based on the Lyapunov characteristic exponent, Melita et al. (2006) separate the Trojan population into sub-populations. The unstable, or transitional, sub-population has $s = -2.25$, while the stable one has a knee in the distribution with a double power law, $s = -4.45$, ($H < 9.41$) and $s = -1.85$, ($H \ge 9.41$). The case of the unstable population is very interesting since this has a higher probability of switching to JFC-like orbits than does the stable one.

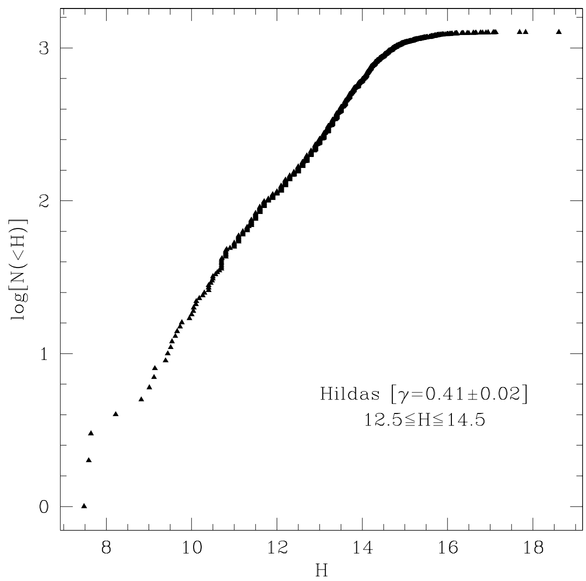

Fig. 4. CLF of Hilda asteroids. The γ-index was obtained in the magnitude range $12.5 \le H \le 14.4$.

Table 1. Indexes of ACOs and related populations.

Pop.	γ	s
ACO (all)	0.51	−2.55
ACO (NEO)	0.44	−2.2
ACO (non-NEO)	0.49	−2.45
Trojans[a]	0.4	−2.0
Trojans[b]	0.38	−1.9
Trojans[c]	0.45	−2.25
Hildas	0.42	−2.1
JFCs[d]	0.53	−2.65

[a] Jewitt et al. (2000). [b] Yoshida & Nakamura (2005). [c] Unstable Trojans, Melita et al. (2006). [d] Tancredi et al. (2006).

Jupiter family comets: the CLF of JFCs has been a subject of intense discussion. Diverse authors obtained different indexes (Lowry et al. 2003; Neslušan 2003; Weissman & Lowry 2003; Meech et al. 2004; Lamy et al. 2005). Nevertheless, Tancredi et al. (2006) present an extended discussion of the problem and conclude that, using all the datasets presented in other papers in an homogeneous manner, the results are similar. with an extended version of their catalog of nuclear magnitudes (Tancredi et al. 2000), they obtain an index $s = -2.65$. Note that this value is suggestively close to that of the non-NEO sample of ACOs.

From the above discussion we conclude that unstable Trojans and Hildas have s-indexes similar to the NEO population of asteroids in cometary orbits. This suggests that an important fraction could be scattered objects from the outer main belt as indicated by Fernández et al. (2002).

On the other hand, the higher slope of non-NEO size distribution argues against a major contribution from the Hildas or Trojans to this population. Their s-index is similar to that of the JFC, suggesting a possible genetic relationship. Therefore, the JFC can be an important source of the non-NEO population. Of course, this does not discard the possible contribution from the other related populations.

5. Conclusions

We computed the cumulative size distribution of asteroids in cometary orbits and its two sub-populations. Significant differences between them have been found, mainly that the NEOs have a shallower s-index. Comparison with related populations suggests different sources that contribute to the sub-populations. In particular the index of the non-NEOs is similar to that of the Jupiter family comets.

The main results can be summarized as:

1. The index of the cumulative size distribution of the ACO population is $s = -2.55 \pm 0.04$. The population can be separated into two sub-samples with significant differences between them. The NEO and non-NEO have cumulative indexes of -2.20 ± 0.04 and -2.45 ± 0.01, respectively.
2. The CLF of the NEOs has an s-index that is different from the Jupiter family comets, pointing to a small contribution from this population. A more significant contribution from the main belt is possible.
3. The similarity of the s-index between non-NEOs and JFCs is consistent with spectroscopic and albedo results and suggests that the latter can be an important source of non-NEOs, although it does not rule out other contributions.

Acknowledgements. We would like to acknowledge D. Lazzaro for useful comments on the draft, G. Tancredi and J. Fernández for kindly providing the list of orbital elements of comets, and an anonymous referee for the constructive comments. AAC would like to thank the Conselho Nacional de Desenvolvimento Científico e Tecnólogico (CNPq) – Brazil, which supported this work via a PhD fellowship.

References

Bottke, W. F., Morbidelli, A., Jedicke, R., et al. 2002, Icarus, 156, 399
Bowell, E., Hapke, B., Domingue, D., et al. 1989, Application of photometric models to asteroids, in Asteroids II, eds. R. Binzel, T. Gehrels, & M. Shapley Matthews (Tucson: Univ. of Arizona Press), 524
Bus, S. J., & Binzel, R. P. 2002, Icarus, 158, 146
Di Sisto, R. P., Brunini, A., Dirani, L. D., & Orellana, R. B. 2005, Icarus, 174, 81
Fernández, J. A., Tancredi, G., Rickman, H., & Licandro, J. 1999, A&A, 352, 327
Fernández, J. A., Gallardo, T., & Brunini, A. 2002, Icarus, 159, 358
Fernández, Y., Jewitt, D. C., & Sheppard, S. S. 2005, AJ, 130, 308
Jewitt, D. 2002, AJ, 123, 1039
Jewitt, D. 2005, AJ, 129, 530
Jewitt, D. C., Trujillo, C. A., & Luu, J. X. 2000, AJ, 120, 1140
Kaasalainen, M., Torppa, J., & Muinonen, K. 2001 Icarus, 153, 37
Kresák, L. 1979, Dynamical interrelations among comets and asteroids, in Asteroids, ed. T. Gehrels (Tucson: Univ. Arizona Press), 289
Lamy, P. L., Toth, I., Fernández, Y. R., & Weaver, H. A. 2005, The sizes, shapes, albedos, and colors of cometary nuclei, in Comets II, ed. M. C. Festou, H. U. Keller, & H. A. Weaver (Tucson: Univ. Arizona Press), 223
Licandro, J., Campins, H., Hergenrother, C., & Lara, L. M. 2002, A&A, 398, L45
Licandro, J., de León, J., Pinilla, N., & Serra-Ricart, M. 2005, Adv. Space Res., in press
Lowry, S. C., Fitzsimmons, A., & Collander-Brown, S. 2003, A&A, 397, 329
Meech, K. J., Hainaut, O. R., & Marsden, B. G. 2004, Icarus, 170, 463
Melita, M., Licandro, J., & Williams, I. 2006, submitted to Icarus
Neslušan, L. 2003, Contrib. Astron. Obs. Skalnaté Pleso, 33, 5
Rickman, H., Fernández, J., & Gustafson, B. 1990, A&A, 237, 524
Tancredi, G., Fernández, J., Rickman, H., & Licandro, J. 2000, A&AS, 146, 73
Tancredi, G., Fernández, J., Rickman, H., & Licandro, J. 2006, Icarus, 182, 527
Weissman, P. R., & Lowry, S. C. 2003, 34th Ann. Lunar Planetary and Science Conf. Abs. No. 2003
Yoshida, F., & Nakamura, T. 2005, ApJ, 130, 2900